Molecular above-threshold-ionization spectra: The effect of moving nuclei

Andre D. Bandrauk,* S. Chelkowski, and Isao Kawata†
Université de Sherbrooke, Quebec J1K 2R1, Canada
(Received 28 May 2002; published 23 January 2003)

Exact non-Born-Oppenheimer simulations of a one-dimensional model of one-electron H_2^+ and linear H_3^{2+} in an intense short laser pulse are used to investigate the nonlinear multiphoton electron emission spectra, called above threshold ionization (ATI). Due to the rapid proton motion on near-femtosecond time scale, the ATI spectra are found to be produced at the critical internuclear distance $R_c \sim 7-8$ a.u., leading to charge-resonance-enhanced ionization (CREI). As a consequence, maxima in the ATI spectra are displaced with respect to the similar H-atom spectra by a laser-induced Stark energy $E_M R_c/2$, where E_M is the maximum amplitude of the laser field. Highly oscillating ATI spectra occur, which are enhanced by the nuclear motion. These are interpreted as due to coherent excitations of the lowest unoccupied molecular orbitals and highest occupied molecular orbitals, which are also responsible for CREI. Electron rescattering effects in the energy regions of $10U_p$ and $8U_p$, where U_p is the ponderomotive energy, are shown to be substantially reduced due to the rapid molecular dissociation and Coulomb explosion. Nevertheless, the ATI spectra in these energy regions reflect the different electron energies in the rescattering process. Fine structures of the ATI spectra are found to be enhanced by moving nuclei, reflecting the enhancement of resonant transitions by varying Franck-Condon factors during the nuclear motion.

DOI: 10.1103/PhysRevA.67.013407 PACS number(s): 32.80.Rm, 42.65.Re, 42.65.Ky

I. INTRODUCTION

Current laser technology is advancing steadily so that high-intensity ($I \geqslant 10^{14}$ W/cm^2), short ($\tau \leqslant 5$ fs) pulses are now becoming standard experimental tools [1]. Most of the attention to the new science of nonlinear laser-matter interactions has been focused on atoms [2], whereas nonlinear laser-molecule interaction is emerging as a new area of research. In the latter, nonlinear phenomena, such as above-threshold dissociation (ATD) [3] and laser-induced molecular potentials [4] have already been explained by a previous nonperturbative approach based on dressed molecule states [5]. With higher intensities, ionization becomes an additional nonperturbative process, leading to many multiphoton transitions that can no longer be treated by simple Fermi–golden-rule formulas. Nonlinear ionization processes are usually accompanied by dissociation, so that *dissociative ionization* needs to be correctly treated in a nonperturbative, non-Born-Oppenheimer framework. We have initiated such a computational program on the simplest one-electron molecule H_2^+, which can be solved exactly numerically [6,7] with state of the art supercomputers. This has led us to the discovery of new nonperturbative, nonlinear laser-molecule effects such as charge-resonance-enhanced ionization (CREI) [8] and molecular high-order harmonic generation (MHOHG) [9], which have no simple perturbative explanation.

The first detailed analysis of nonlinear multiphoton electron spectra, called above-threshold-ionization (ATI) spectra in analogy with the atomic case [2], were performed for the H_2 molecule [10,11]. The observed photoelectron energy spectra resulting from multiphoton processes in H_2 showed clear nonperturbative radiative effects between the perturbed molecular states of H_2^+, in particular, including a dissociative state. These effects were interpreted in terms of the theory of the dressed states of this ion [3,5]. Such states did not include further dissociative ionization of the ion itself leading to Coulomb explosion.

In the present paper, we return to a complete non-Born-Oppenheimer simulation of dissociative ionization of the one-electron system, H_2^+ and H_3^{2+}. We restrict ourselves to linear one-dimensional (1D) models that can be solved exactly and that can reproduce faithfully electron-proton kinetic-energy coincidence experiments for low-frequency (long-wavelength) cases ($\lambda = 800, 1064$ nm). As shown in detail recently for the atomic case, despite the complexity of the high-intensity regime, a very small number of clearly identified quantum orbits is sufficient to describe ATI and higher-order harmonic generation (HOHG) processes [12,13], in agreement with a simple quasistatic model of atomic tunneling ionization [14]. The extension of these simple atomic pictures to molecules is the main goal of the present work. In our previous calculations with static nuclei, we did exact nonperturbative (i.e., Born-Oppenheimer) simulations of molecular ATI [15] and which led to the proposal of laser-induced electron diffraction (LIED) as a new tool for probing ultrafast molecular dynamics. By exact calculations, the present paper examines the effect of the nuclear motion and therefore non-Born-Oppenheimer effects on LIED for the one-electron system H_2^+ and linear H_3^{2+}. Our recent work in this direction has shown that intense, ultrashort IR and UV laser pulses can lead to dynamic imaging of nuclear wave functions [16,17]. Our goal in this paper is to clarify

*Present address: Canada Research Chair in Computational Chemistry and Photonics.
Electronic address: andre.bandrauk@courrier.usherb.ca
†Present address: Department of Chemical System Engineering, Graduate School of Engineering, The University of Tokyo, Tokyo 113-8656, Japan.

the electronic and nuclear correlation dynamics by investigating the characteristic features of ATI molecular spectra in the long-wavelength region ($\lambda = 800,1064$ nm) since the current ultrashort intense laser-pulse technology is well developed in this long-wavelength regime and offers many new applications for intense ultrashort laser pulses [1].

The rest of this paper is organized as follows. In Sec. II, we summarize the numerical method for solving the time-dependent Schrodinger equation (TDSE). In Sec. III, we present numerical results on nonlinear multiphoton electron or ATI spectra of H_2^+ and H_3^{2+}, and finally in Sec. IV we present a recollision model that gives a clear interpretation to the characteristics of molecular ATI spectra with moving nuclei.

II. NUMERICAL METHODS

Photoionization of molecules is expected to produce interference patterns following a simple Born-Oppenheimer approximation calculation depending on fixed internuclear distance R and the ejected electron momentum p [18,19]. High-order nonlinear terms have to be considered in the multiphoton regime [15,20]. In the present work, we assume that the molecule is aligned parallel to the laser field, which is known to occur at high intensities [21]. We therefore examine numerically nonlinear photoionization or ATI spectra in a 1D model, which is expected to reproduce at low frequencies the essential dynamics due to the presence of more than one nucleus as compared to atoms. This would correspond to the experimentally measured spectra parallel to the incident, linearly polarized laser field. We follow the numerical treatment described in our previous 1D calculations [7,17], which have been calibrated against our previous 3D simulations of H_2^+ [6] for consistency.

We solve numerically the complete 1D TDSE for moving electrons and nuclei. The model we employ here is a 1D one, in which the electron moves along the molecular axis, and the molecular axis is parallel to the polarization direction of the field. For the H_2^+ 1D model, the TDSE is given by the following form (throughout this paper atomic units are used, $e=\hbar=m_e=1$):

$$i\frac{\partial}{\partial t}\psi(z,R,t) = H(z,R,t)\psi(z,R,t), \tag{1}$$

where

$$H(z,R,t) = H_N(R) + H_{el}(z,R,t), \tag{2}$$

$$H_N(R) = -\frac{1}{m_p}\frac{\partial^2}{\partial R^2} + \frac{1}{R}, \tag{3}$$

$$H_{el}(z,R,t) = -\beta\frac{\partial^2}{\partial z^2} + V_C(z,R) + \kappa z E(t), \tag{4}$$

$$\beta = -\frac{2m_p + m_e}{4m_p m_e}, \quad \kappa = 1 + \frac{m_e}{2m_p + m_e}, \tag{5}$$

$$V_C(z,R) = -[1+(z-R/2)^2]^{-1/2} - [1+(z+R/2)^2]^{-1/2}. \tag{6}$$

Here, m_e and m_p are the electron and proton masses ($m_e = 1$, $m_p = 1837$), respectively. The Hamiltonian (2) is the exact 1D three-body expression one obtains after the separation of the center-of-mass motion [22] with regularized Coulomb potential (6) that is introduced to reproduce correct ionization potentials. For H_3^{2+}, the corresponding Hamiltonian can be found in our previous work on this molecule in Refs. [23,24], and in this case we consider only symmetric stretching for nuclear motion expected in the Coulomb explosion. The numerical solution of the TDSE (2) is obtained by an iterative procedure based on a high-order split-operator method that preserves unitarity at each time step of the iteration [25]. A two-box procedure is used, i.e., an internal box of size $|z| \leqslant 500$ a.u.. is used to calculate the exact time-dependent wave function ψ_{in} which is then projected onto Volkov states (the exact solution of a free electron in a laser pulse [7,26]) for $|z| > 500$ a.u. The latter are propagated well past the end of the pulse. Total pulse durations are usually 20 cycles with a five-cycle rise and fall. After integration over the nuclear coordinate R, one recovers the asymptotic total electron probability distribution in momentum space $f(p,t_f)$ for a final time $t_f > t_p$, where t_p is pulse length, since the Volkov states are most readily expressed in momentum space. The initial wave function at $t=0$ is assumed to be in the following form:

$$\psi(z,R,0) = \chi(R)\phi_0(R,z), \tag{7}$$

where $\phi_0(R,z)$ is the field-free initial eigenfunction of the electronic Hamiltonian H_2^+ or H_3^{2+} at fixed R and $\chi(R)$ is the initial nuclear wave function, either for an initial vibrational state $\chi_v(R)$ of quantum number v or a Frank-Condon superposition of $\chi_v(R)$'s, which is expected to be created from the initial rapid one-electron ionization of H_2 or H_3^+ in their ground electronic state ($v=0$) at equilibrium internuclear distance R_e, respectively.

In order to confirm the consistency of the two-box procedure, i.e., projection of the exact internal wave function $\psi_{in}(z,R,t)$ onto Volkov states in the length-gauge calculations based on the Hamiltonian (2), the same calculations were performed in the Bloch-Nordsieck [5], or equivalently, space-translation gauge [27]. In this new representation, the field term $\kappa z E(t)$ [in Eq. (4)] is eliminated by a unitary transformation and now appears as a modified Coulomb potential,

$$V_C = V_C(z-\alpha(t),R), \tag{8}$$

where

$$\alpha(t) = \kappa\int_0^t ds\int_0^s d\tau E(\tau). \tag{9}$$

The advantage of this new gauge is that contrary to the divergent length-gauge radiative term $\kappa z E(t)$ in Eq. (4), radiative terms vanish in Eq. (8) asymptotically ($|z|\to\infty$), and projections of the internal wave function ψ_{in} are now made

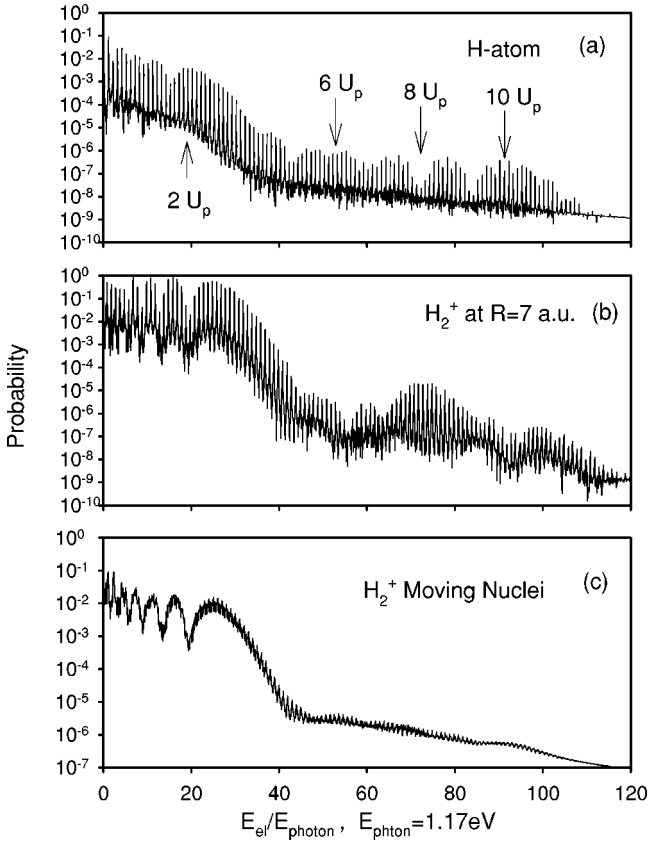

FIG. 1. ATI electron spectra as functions of electron energy/photon energy, for $\lambda = 1064$ nm, at $I = 1.0 \times 10^{14}$ W/cm^2, generated by (a) 1D hydrogen atom, (b) H_2^+ for R fixed at $R_c = 7$ a.u., and (c) H_2^+ with moving nuclei. In the case of (c), $\chi(R)$ in the initial wave function expressed by Eq. (7) is for a Frank-Condon superposition of $\chi_v(R)$.

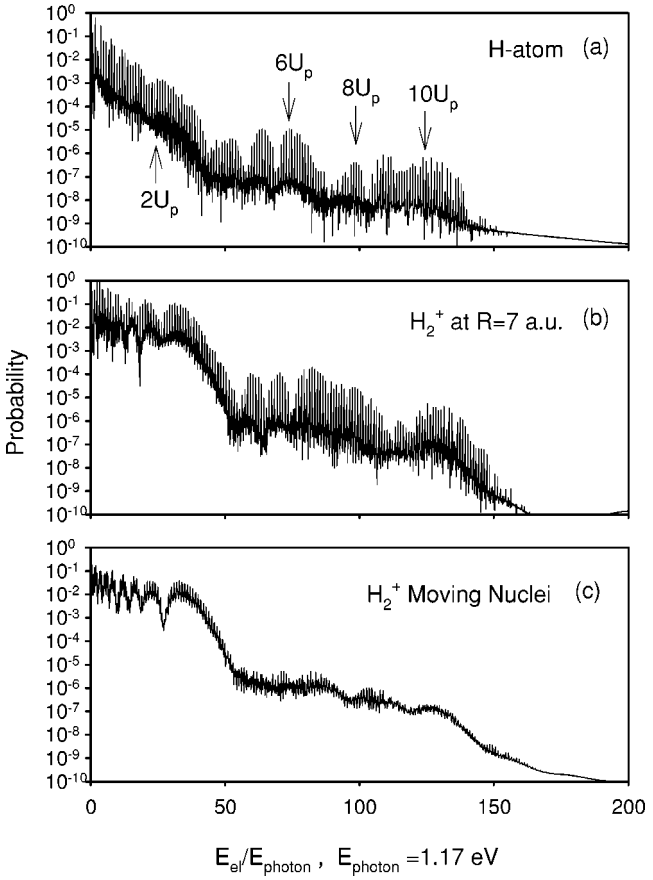

FIG. 2. ATI electron spectra as functions of electron energy/photon energy, for $\lambda = 1064$ nm, at $I = 1.4 \times 10^{14}$ W/cm^2, generated by (a) 1D hydrogen atom, (b) H_2^+ for R fixed at $R_c = 7$ a.u., and (c) H_2^+ with moving nuclei. In the case of (c), $\chi(R)$ in the initial wave function expressed by Eq. (7) is for a Frank-Condon superposition of $\chi_v(R)$.

simply onto the free-electron Coulomb states. All calculations presented below were performed in both gauges, thus confirming the accuracy of the numerical procedure for non-Born-Oppenheimer electron-nuclear dynamics in dissociative-ionization processes at high intensities.

III. NONLINEAR MULTIPHOTON ELECTRON OR ATI SPECTRA OF H_2^+ AND H_3^{2+}

Using the numerical procedure described in the preceding section, we present in Figs. 1–6 the calculated ATI spectra for 20-cycle laser pulses of wavelengths $\lambda = 1064$ nm ($\omega = 0.043$ a.u.) and $\lambda = 800$ nm ($\omega = 0.057$ a.u.), and the peak intensities $I = 1 \times 10^{14}$ W/cm^2 [$E_M = (8\pi I/c)^{1/2} = 0.053$ a.u., where E_M is the the peak value of the electric field], $I = 1.4 \times 10^{14}$ W/cm^2 ($E_M = 0.067$ a.u.), $I = 2.0 \times 10^{14}$ W/cm^2 ($E_M = 0.075$ a.u.), and finally $I = 4.0 \times 10^{14}$ W/cm^2 ($E_M = 0.106$ a.u.), respectively. For each intensity, we present (a) the ATI spectrum of a single H atom, (b) H_2^+ at $R = 7$ a.u., and finally (c) H_2^+ with moving nuclei, i.e., the last one is the exact 1D non-Born-Oppenheimer simulation of the dissociative ionization process; (b) corresponds to the critical internuclear distance R_c where CREI occurs. Around this R_c ionization rates of molecular ions exceed that of the dissociated fragments (i.e., atoms) by at least one order of magnitude, as shown in exact simulations for one electron [6,8], and recently, two-electron systems [23,24].

A first perusal of Figs. 1–6 shows certain similarities and important dissimilarities in the ATI spectra of the H atom compared to that of H_2^+. These spectra are reported in photon number n or photon energies $E_n = n\hbar\omega$. Minima and maxima in the intensities occur at various energies, which can be characterized in terms of a plasma physics concept [14], the ponderomotive energy

$$U_p = \frac{(eE_M)^2}{4m\omega^2} = \frac{I}{4\omega^2} \text{ (a.u.)}. \tag{10}$$

This energy is the average classical oscillatory energy acquired by an electron in an electro-magnetic field of intensity $I = cE_M^2/8\pi$, where E_M is the field maximum amplitude. Simple classical models of the motion of an electron in an electromagnetic pulse also allow us to calculate the kinetic energy of the returning electron to the parent ion after tunneling through the barrier near a field maximum. These mod-

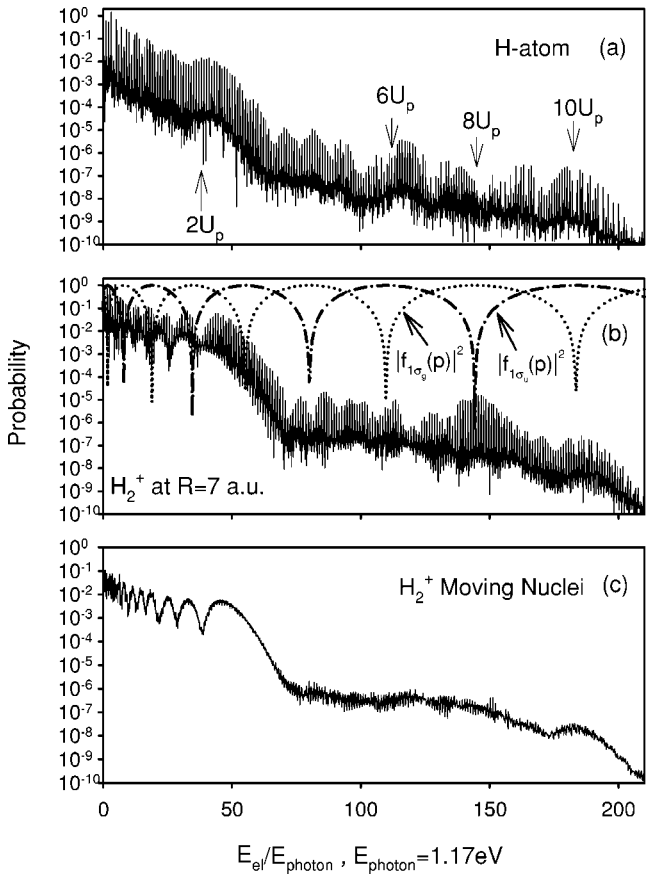

FIG. 3. ATI electron spectra as functions of electron energy/photon energy, for $\lambda = 1064$ nm, at $I = 2.0 \times 10^{14}$ W/cm^2, generated by (a) 1D hydrogen atom, (b) H_2^+ for R fixed at $R_c = 7$ a.u., and (c) H_2^+ with moving nuclei. In the case of (c), $\chi(R)$ in the initial wave function expressed by Eq. (7) is for a Frank-Condon superposition of $\chi_v(R)$.

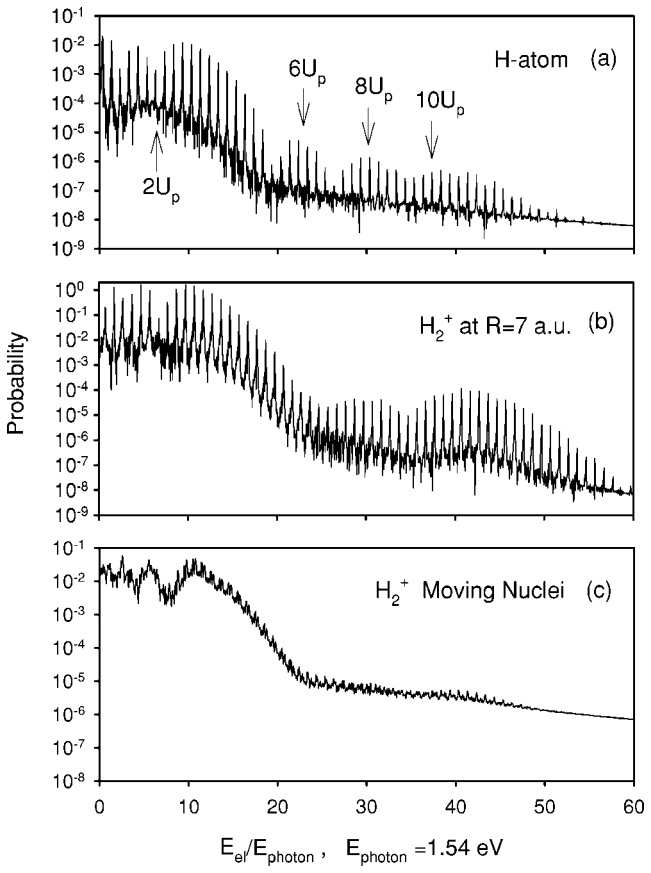

FIG. 4. ATI electron spectra as functions of electron energy/photon energy, for $\lambda = 800$ nm, at $I = 1.0 \times 10^{14}$ W/cm^2, generated by (a) 1D hydrogen atom, (b) H_2^+ for R fixed at $R_c = 7$ a.u., and (c) H_2^+ with moving nuclei. In the case of (c), $\chi(R)$ in the initial wave function expressed by Eq. (7) is for a Frank-Condon superposition of $\chi_v(R)$.

els predict that the maximal energy of the returning electron is $3.17U_p$ [9,14]. We shall adopt the value πU_p which agrees with our molecular HOHG calculations [9]. The corresponding wavelength λ_r of such a rescattering electron that is expected to *diffract* by recollision with the ion core is readily calculated to be for the recollision momentum $p_r = (2\pi U_p)^{1/2}$,

$$\lambda_r = \frac{2\pi}{p_r} = (2\pi/U_p)^{1/2}. \tag{11}$$

We tabulate in Tables I and II the values of U_p and λ_r for the intensities and wavelengths used in Figs. 1–6.

The critical internuclear distances R_c for maximum ionization can be derived from a quasistatic model of tunneling ionization and correspond to the internuclear distances where the electron in the Stark-shifted lowest unoccupied molecular orbital (LUMO) undergoes overbarrier ionization in the presence of the Coulomb potential $V_C(z,R)$ and the Stark energy, $-\kappa z E_M$ in Eq. (4). This results in $R_C \simeq 4/I_p$, where I_p ($=0.67$ a.u.) is the ionization energy of 1D H atom, and R_c turns out to be relatively independent of the laser intensity I around the range 10^{14} W/cm^2 [8,28]. This is confirmed by investigating not only the ATI spectra of the static nuclei ($R_c = 7$ a.u.), calculations shown in Figs. 1(b)–6(b), but also those of the exact non-Born-Oppenheimer calculations with moving nuclei shown in Figs. 1(c)–6(c). The outstanding difference between the ATI spectra of the static nuclei at $R_c = 7$ a.u. and those of the exact moving nuclei is the fine structure of the ATI peaks seen in the latter case, namely, the non-Born-Oppenheimer case. This fine structure, not present in the static (Born-Oppenheimer) results, is suggestive of different resonance energies acquired by the moving nuclei during the dissociative-ionization process around the critical distance R_c for CREI. This will be addressed in the last paragraph of the following section.

A first indication of molecular structure on the ATI peaks can be observed by comparing the spectra of H atom in Figs. 1(a)–6(a) with those of H_2^+ with static nuclei ($R_c = 7$ a.u.) in Figs. 1(b)–6(b), and also with those of H_2^+ with moving nuclei in Figs. 1(c) and 6(c). The maximum beyond $2U_p$ preceded by a minimum at $1.65U_p$ is shifted to higher energies in the molecular case when compared to the H-atom results. As explained below, this is due to ''up-field excitation'' of electrons in the molecular case which has no counterpart in atoms. A clear cutoff in the kinetic-energy spectra

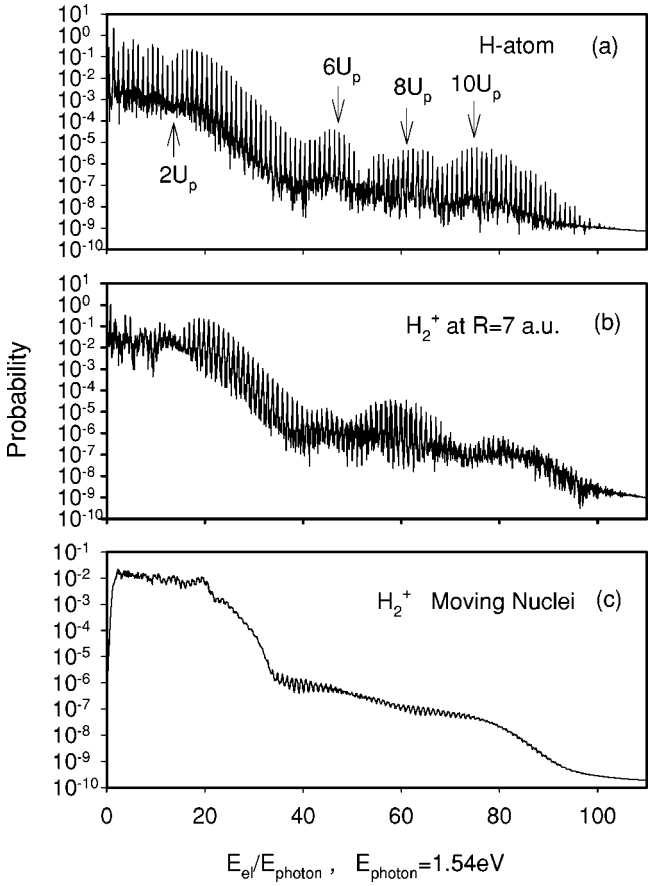

FIG. 5. ATI electron spectra as functions of electron energy/photon energy, for $\lambda = 800$ nm, at $I = 2.0 \times 10^{14}$ W/cm^2, generated by (a) 1D hydrogen atom, (b) H_2^+ for R fixed at $R_c = 7$ a.u., and (c) H_2^+ with moving nuclei. In the case of (c), $\chi(R)$ in the initial wave function expressed by Eq. (7) is for an initial vibrational state $\chi_v(R)$ $(v=0)$.

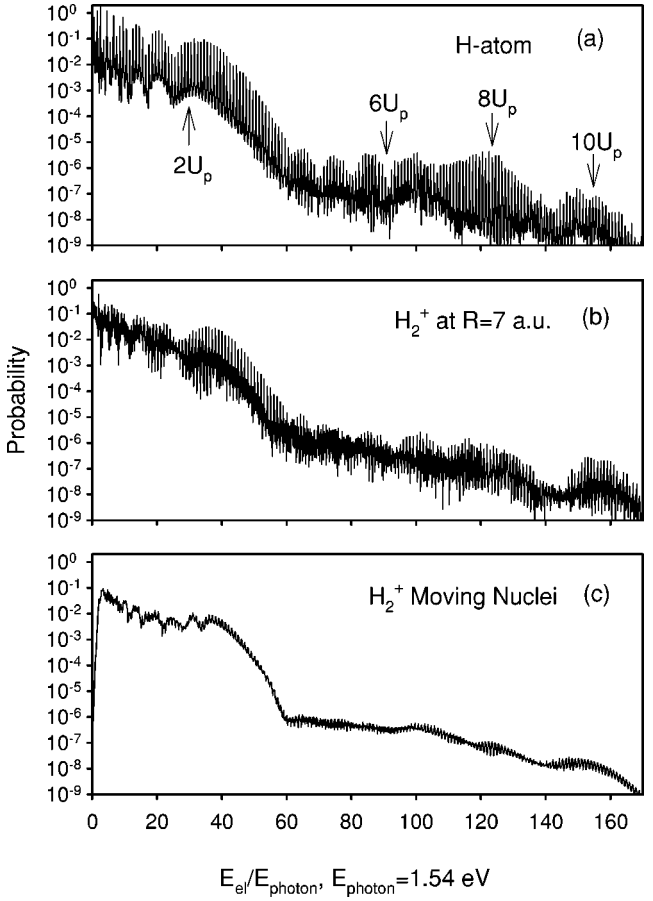

FIG. 6. ATI electron spectra as functions of electron energy/photon energy, for $\lambda = 800$ nm, at $I = 4.0 \times 10^{14}$ W/cm^2, generated by (a) 1D hydrogen atom, (b) H_2^+ for R fixed at $R_c = 7$ a.u., and (c) H_2^+ with moving nuclei. In the case of (c), $\chi(R)$ in the initial wave function expressed by Eq. (7) is for an initial vibrational state $\chi_v(R)$ $(v=0)$.

occurs with a maximum around $2U_p$ preceded by a minimum at $1.65U_p$ for the H atom for all three intensities. Such $2U_p$ electrons have been identified from semiclassical path-integral calculations as *direct* electrons [12], which were already predicted earlier from simple tunneling ionization models [14]. This $2U_p$ energy maximum is consistently shifted by the energy $E_M R_c/2$ (see Table I) in the case of H_2^+, with $R_c \simeq 7$ a.u. The energy $E_M R_c/2$ is precisely the Stark shift of the LUMO due to the charge-resonance effects in symmetric ions such as H_2^+ [8,28,29], and is responsible for the enhanced ionization at $R_c \simeq 7$ a.u. Thus in molecular ions such as H_2^+, charge-resonance effects increase the energy of the outgoing electron at the critical distance R_c by the energy $E_M R_c/2$, which is the radiative coupling of the HOMO (highest occupied molecular orbital)-LUMO transition at the peak field strength E_M. It is to be noted that this is equivalent to the potential-energy increase of the electron transferred by the field to the distance R_c of the up-field proton, thus confirming the applicability of simple quasistatic models from atoms [8] to molecules [28]. This is also consistent with studies of the electron excitations mechanism that shows that the ionizing electron is ejected ''up-field,'' i.e., with the higher potential energy $E_M R_c/2$, [24,29]. This differs from atoms where overbarrier ionization would be expected to occur at the present field strength $E = 0.045$ a.u. [1,14]. Indeed, this is the fundamental difference between atoms and molecules due to the presence of a strong HOMO-LUMO radiative coupling between these in the molecules.

A more prominent difference between the ATI spectra of H atom [Figs. 1(a)–6(a)] and those of H_2^+ molecule [from Figs. 1(b), 1(c) to Figs. 6(b), 6(c)] is the appearance of additional oscillations in the molecular ATI spectra. In the molecular case, the similarities between the spectra of the static nuclei fixed at $R_c = 7$ a.u. and those of the moving nuclei is clear, with the minima and maxima occurring at the same energies in both cases, thus confirming that ionization is indeed occurring around $R \simeq R_c$, and its rate is much faster than that of dissociation. We can justify this fact that ionization (electron) dynamics can be almost determined around the critical internuclear distance R_c by referring to our previous paper in Ref. [7]. In this paper one can see a great difference in ATI spectra for $R = R_e = 7.6$ a.u. (Fig. 10) and $R = 29$ a.u. (Fig. 11). In the case of H_2^+, the dissociation is

TABLE I. Laser and physical parameters for $\lambda = 1064$ nm ($\omega = 0.0428$ a.u.) and $R_c = 7$ a.u.

I (W/cm^2)	U_p	λ_r (a.u.)	α (a.u.)	$E_M R_c/2$	γ (H_2^+)	R_c/λ_r
1×10^{14}	9.10ω	4.02	29.1	4.37ω	0.93	1.74 (2.12)
1.4×10^{14}	12.6ω	3.41	34.3	5.14ω	0.79	2.05 (2.43)
2×10^{14}	18.2ω	2.83	41.2	6.18ω	0.67	2.46 (2.85)

a rather rapid process which occurs on the time scale around 10 fs. This fact allows the protons to reach the critical internuclear distance R_c during the pulse duration ($\tau \simeq 20$ cycles $\simeq 70$ fs at 1064 nm and 54 fs at 800 nm).

We present similar results for H_3^{2+} at 800 nm in Figs. 7–9. As opposed to the case of H_2^+, where the initial state is a superposition of the bound vibrational states of the ground electronic state $^2\Sigma_g^+$, the ground electronic state of H_3^{2+} is repulsive, so that we initialize the nuclear wave function as a Gaussian wave packet at $R \simeq 5$ a.u., which is the equilibrium internuclear distance of a 1D linear H_3^+. Here we assume that the fast one-electron ionization of H_3^+ occurs at this distance, and H_3^{2+} is created [24]. In the case of H_3^{2+}, simulations have been performed for $\lambda = 800$ nm ($\omega = 0.057$ a.u.) and intensities 1.0×10^{14} W/cm^2, 2.0×10^{14} W/cm^2, and 4.0×10^{14} W/cm^2. The numerical laser parameters are summarized in Table II. Comparison of the ATI spectra maxima at $2U_p$ for the H atom [Figs. 4(a)–6(a)] with the H_3^{2+} spectra obtained at the critical CREI distance $R_c \simeq 8$ a.u. [Figs. 7(a)–9(a)] and the exact spectra for moving nuclei [Figs. 7(b)–9(b)] shows that as in the previous H_2^+ case, Figs. 1–6, $2U_p$ maxima of the H atom are shifted also by the amount $E_M R_c/2$, where E_M is the maximum electric-field amplitude corresponding to the intensities 1.0×10^{14}, 2.0×10^{14} W/cm^2, and 4.0×10^{14} W/cm^2. Alternatively, the minima in the ATI spectra which occur for the H atom between $(1.6–1.8)U_p$ are consistently shifted in all cases by approximately $E_M R_c/2$ in H_3^{2+}.

In order to interpret qualitatively the quantitative results reported in Figs. 1–9, we refer to our previous study of LIED [15], where 2D H_2^+ calculations were performed of ATI spectra for various static internuclear distances. In both short-pulse and long-pulse limits, the structure of the spectra was determined by the momentum space structure of the initial molecular orbital from which the electron is ionized. Thus in the case of H_2^+, both the HOMO ($1\sigma_g$) and LUMO ($1\sigma_u$) need to be considered since at R_c both orbitals are nearly equally populated by the laser field [9,29,30]. We note that recent experimental [31] and theoretical work [20,32] on molecular ATI spectra emphasize the importance of the symmetry of the initial molecular orbital on high intensity ionization rates. In general, the effect of a short pulse is to shift the total momentum distribution by the instantaneous or maximum Stark shift $E_M R_c/2$ [15]. As we have shown in the preceding section, minima and maxima of the ATI spectra of H_2^+ and H_3^{2+} are shifted by this amount with respect to the spectra of an H atom where delocalization of the electron is absent. Thus for the HOMO ($1\sigma_g$) and LUMO ($1\sigma_u$) orbitals, the ionized electron distribution is proportional to the momentum function for parallel field excitation [15],

$$f_{1\sigma_g}(p) \sim \cos[(E_M + p)R/2], \tag{12}$$

$$f_{1\sigma_u}(p) \sim i \sin[(E_M + p)R/2]. \tag{13}$$

Since at $R = R_c$ both orbitals are initially nearly equally populated [9,29], we can expect

$$f(p) = \alpha \cos[(E_M + p)R/2] + \beta i e^{i\phi} \sin[(E_M + p)R/2]. \tag{14}$$

Assuming that $\alpha = \beta$, we have

$$|f(p)|^2 \simeq 1 + \sin[(E_M + p)R_c], \tag{15}$$

with extrema at $(E_M + p)R_c = (2n+1)\pi/2$, minimum for n odd, and maximum for n even. We next test this hypothesis in order to explain the accentuated oscillations of the ATI intensity pattern of H_2^+ as compared to spectra in H atom. It should be noted that the assumption of exact localization of the electron on one proton means $e^{i\phi} = \pm 1$, and this assumption leads to no oscillations. We plot in Fig. 3(b) the factors $|f_{1\sigma_g}(p)|^2$ (dotted line) and $|f_{1\sigma_u}(p)|^2$ (broken line). Comparison with the localized $|f(p)|^2$, Eq. (15), and with exact spectra shows that the exact ATI spectra generally have twice the number of oscillations compared to the localized model. The frequency of ATI oscillations is closer to the model of ionization occurring independently from the HOMO or LUMO. This doubling of the frequency can be observed if $\alpha \neq \beta$, implying a coherent superposition of HOMO and LUMO.

TABLE II. Laser and physical parameters for $\lambda = 800$ nm ($\omega = 0.057$ a.u.) and $R_c = 8$ a.u.

I (W/cm^2)	U_p	λ_r (a.u.)	α (a.u.)	$E_M R_c/2$	γ (H_2^+)	R_c/λ_r
1×10^{14}	3.86ω	5.34	16.5	3.75ω	1.23	1.50 (2.10)
2×10^{14}	7.73ω	3.77	23.3	5.31ω	0.87	2.11 (2.75)
4×10^{14}	15.5ω	2.67	33.0	7.51ω	0.62	3.00 (3.65)

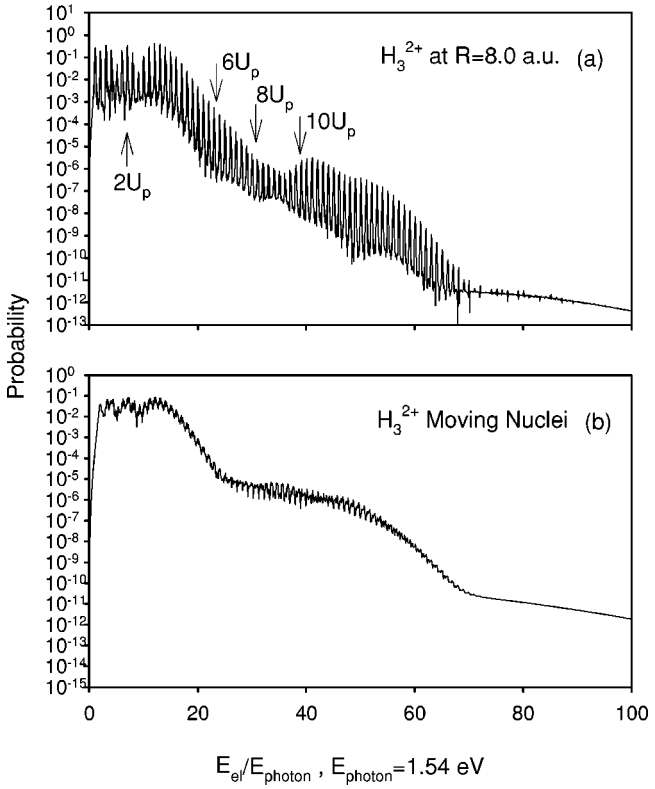

FIG. 7. ATI electron spectra of linear H_3^{2+} as functions of electron energy/photon energy, for $\lambda = 800$ nm, at $I = 1.0 \times 10^{14}$; (a) R fixed at $R_c = 8$ a.u., and (b) with moving nuclei.

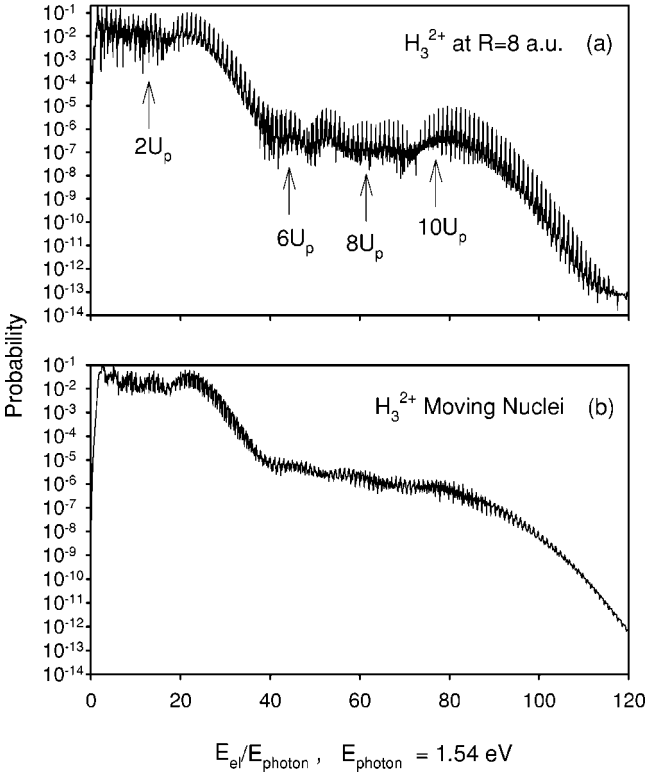

FIG. 8. ATI electron spectra of linear H_3^{2+} as functions of electron energy/photon energy, for $\lambda = 800$ nm, at $I = 2.0 \times 10^{14}$; (a) R fixed at $R_c = 8$ a.u., and (b) with moving nuclei.

IV. RECOLLISION MODEL

A fundamental concept of the ionization of atoms under low-frequency, high-intensity laser fields is the recollision of the ionized electron with the ion core [14]. It has been proven that this concept is useful for the explanation of the ''cutoff'' in atomic HOHG. We have shown that in molecules the ionized electron can recollide with a neighboring atom, thus extending HOHG plateaus to even higher energies at large internuclear distances [9]. Figures 1–9 have shown that ionization occurs at the critical distance $R_c \approx 7$–8 a.u. for CREI due to the very fast dissociation of H_2^+ and H_3^{2+} caused by the field-induced transitions between the HOMO $(1\sigma_g)$ and the LUMO $(1\sigma_u)$. As pointed out in Sec. III, considerable fine structure can be seen in the ATI spectra of the moving nuclei. They appear as amplification of the fine structure already occurring in the ATI spectra at the fixed critical internuclear distance R_c. In view of the fact that similar structures occur in the ATI spectra of the unstable H_3^{2+} system (Figs. 7–9) as in the stable H_2^+ system (Figs. 1–6), one can conclude that these interferences are due to electronic effects as a result of the coherent excitations between the LUMO and HOMO by the laser field, as described in Eq. (14). On the basis of the simple recollision model [14,33] we infer that the maximum kinetic energy should occur at recollision for a field $E(t) = E_0 \cos(\omega t + \phi)$ at the phases $\phi = 0.1\pi, \omega t = 1.30\pi$, resulting in the recolliding energy πU_p for which we have calculated the recollision wavelength λ_r of such an electron in Tables I and II according to Eq. (11). The corresponding asymptotic energy of the ejected electron is $10.2U_p$ [33], whereas the maximum kinetic energy of the ionized electron without recollision with the core or with collision with neighboring atom becomes $8U_p$ [9]. All spectra illustrated in Figs. 1–9 indeed show well-defined maxima at $\sim 8U_p$ and $10U_p$ especially in the case of H atom and H_2^+ with the fixed internuclear distance at R_c. Nuclear motion due to Coulomb explosion $(A_2^+ \rightarrow H^+ + H^+ + e^-)$ has the effect of flattening plateaus, i.e., equalizing intensities of ATI peaks. Three different types of structured ATI peaks appear: (a) (2–3) U_p corresponding to direct ionization, (b) $8U_p$ corresponding to the maximum energy electron without recollision, and finally (c) $10U_p$, where electrons with kinetic energy πU_p recollide with the Coulomb exploding H^+H^+ or $H^+H^+H^+$ core. Further recollision can asymptotically produce electrons with kinetic energies $8.8U_p$ (second recollision with $2.4U_p$ at the nucleus) and $8.5U_p$ (third recollision with kinetic energy $2.25U_p$ at the nucleus) [33]. We assume that these further recollisions are negligible due to the rapid movement and displacement of the protons by Coulomb explosion that occurs on femtosecond time scale as shown below.

As discussed in the preceding section, the first cutoff in the ATI spectra of H_2^+ and H_3^{2+} around $2U_p$ is shifted with respect to the H atom spectra by the energy of the Stark-shifted LUMO, $E_M R_c/2$, as tabulated in Tables I and II. This is indicative of the laser-induced excitation of the ionized electron from the HOMO to the LUMO, with the result that the tunneling electron must leave at the highest potential-

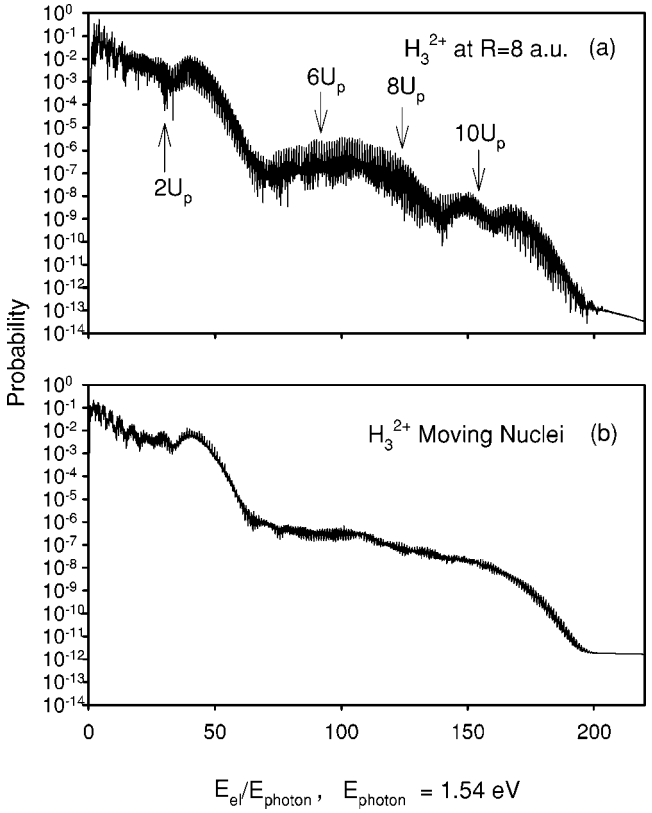

FIG. 9. ATI electron spectra of linear H_3^{2+} as functions of electron energy/photon energy, for $\lambda=800$ nm, at $I=4.0\times10^{14}$; (a) R fixed at $R_c=8$ a.u., and (b) with moving nuclei.

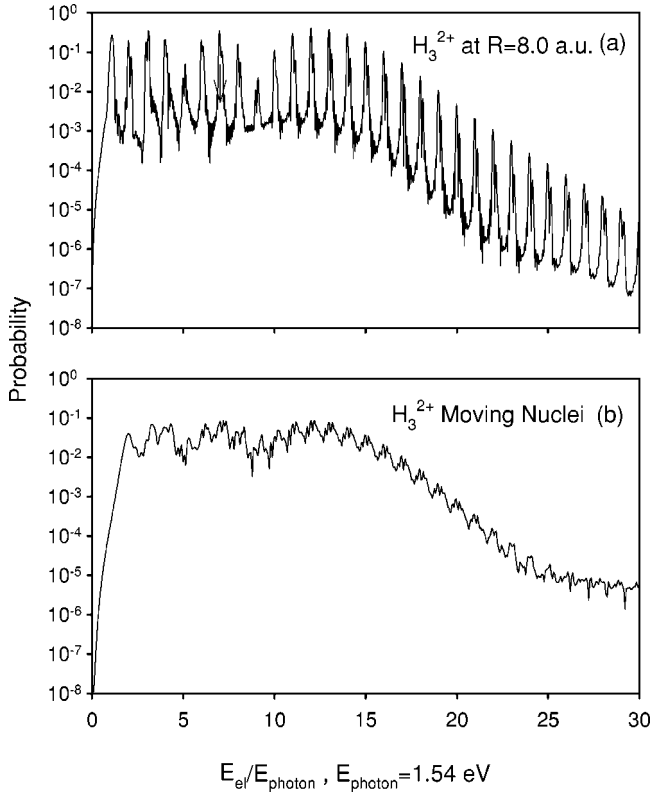

FIG. 10. Detailed ATI spectra for H_3^{2+} at $\lambda=800$ nm and $I=1.0\times10^{14}$ W/cm^2; (a) fixed nuclei at $R=8$ a.u. and (b) moving nuclei.

energy end of the molecule, i.e., upfield. This has been corroborated by detailed calculations for one-electron system [29,34,35] and even for two-electron systems [24]. In the ultrashort pulse (δ-function) limit, this effect appears in Eqs. (12)–(15) as a field-induced phase shift, $E_MR/2$, corresponding to a momentum change $\Delta p=E_M$ in the ionization amplitude. In the standard recollision model applied to atoms [14,33], the maximum measurable asymptotic ATI energy at $10.2U_p$ is obtained by electrons that have recollided at the nucleus with πU_p energy, with a wavelength $\lambda_r=(2\pi U_p)^{1/2}$, Eq. (11). We have tabulated this formula in Tables I and II, in addition to the oscillatory (ponderomotive) radius $\alpha=E/\omega^2$ of an electron in a field of amplitude E and frequency ω. We also have added the Keldysh parameter $\gamma=(I_p/2U_p)^{1/2}$ for H_2^+ with I_p, the H_2^+ ionization potential of an H atom calculated at the CREI distance R_c, namely, $I_p\simeq-0.67-1/R_c$ a.u. This parameter serves to separate the tunneling ($\gamma<1$) from the multiphoton ionization regime ($\gamma>1$) [14]. Thus from Tables I and II, we observe that at $\lambda=1064$ nm, $I=2.0\times10^{14}$ W/cm^2 and $\lambda=800$ nm, $I=4.0\times10^{14}$ W/cm^2, we expect to have tunneling ionization, whereas at lower intensities, one is at the frontier of both regimes.

We first note that in all cases, $\alpha\gg\lambda,R_c$, so that recollision with the neighboring nucleus at distance $R=\pi\alpha$, which occurs at phase $\omega t=\pi$ with energy $8U_p$ [9] is not present. Second, if recollision of the electron occurs with the core at R_c with the energy πU_p, i.e., electron wavelength $\lambda_r=(2\pi U_p)^{1/2}$, one should observe recollision diffraction effects due to the presence of the two-proton scattering centers separated by distance R. In the ultrashort pulse limit, i.e., $\tau_L\ll2\pi/\omega$, such recollision diffraction cannot occur and only the direct ionization phase interference effect, $E_MR/2$ [Eqs. (12)–(15)], appears. In the longer pulse limit, where the field acts on the ionized electron and assists it in the recollision, we should expect a phase change $\Delta\phi=PR=2\pi R/\lambda_r$ to occur at high energies, especially at energy πU_p. Since at the recollision time, the amplitude of the laser field is nearly zero [33], then one can model the returning electron as scattered by a 1D well of dimension R. This results in reflection and transmission probabilities, given by

$$P_r=\frac{\sin^2(PR)}{\sin^2(PR)+4E(E-V_0)/V_0^2}, \tag{16}$$

$$P_t=\frac{4E(E-V_0)/V_0^2}{\sin^2(PR)+4E(E-V_0)/V_0^2}, \tag{17}$$

where E is the kinetic energy with respect to the minimum of the well of depth V_0 [36]. When $PR=n\pi$, i.e., whenever $R/\lambda_r=n/2$, where n is an integer, there is minimum reflection and maximum transmission, meaning that there is no interference, or equivalently, no rescattering. In Tables I and II, we have given the ratio R_c/λ_r, assuming that recollision occurs at $R=R_c$ with energy πU_p. Thus for most of the

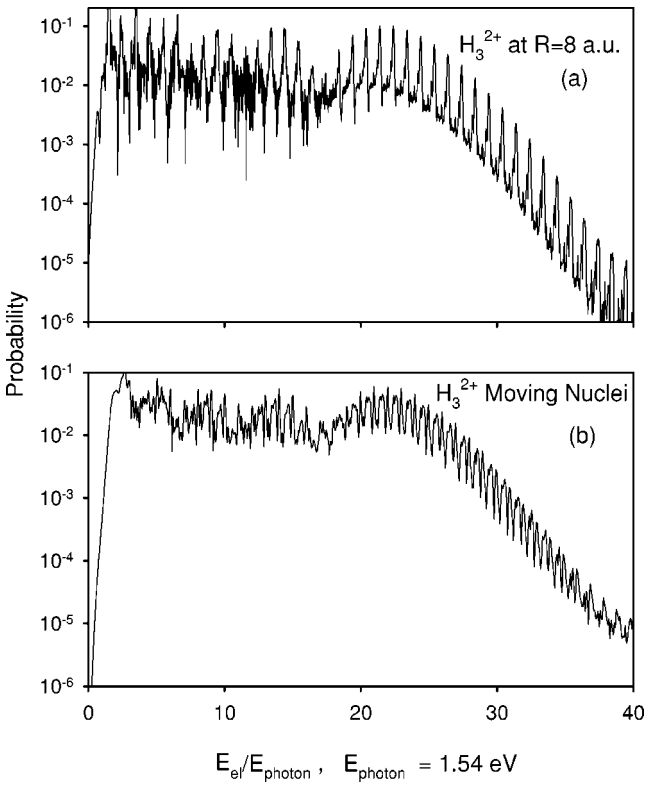

FIG. 11. Detailed ATI spectra for H_3^{2+} at $\lambda=800$ nm and $I=2.0\times10^{14}$ W/cm^2; (a) fixed nuclei at $R=8$ a.u. and (b) moving nuclei.

wavelengths and intensities appearing in these tables, we expect maximum transmission and little reflection, so that the $10U_p$-energy electrons should have maximum intensity. The addition of the extra initial Stark energy $E_M R_c/2$ acquired by the ionizing electron as it leaves from the Stark-shifted LUMO only changes the ratio R/λ_r by about 20–30 % (see numbers in parentheses). In conclusion of this section, a comparison of the ATI spectra intensities reveals little information about recollision diffraction. As an example, we have included in Table I (1064 nm) the intensity 1.4×10^{14} W/cm^2 for which $R/\lambda_r\simeq2$, as compared to intensity 2×10^{14} where $R/\lambda_r\simeq2.5$. Both ATI spectra (Figs. 2 and 3) are quite similar.

Thus in the H atom, $8U_p$ and $10U_p$ have similar probabilities [Figs. 1(a)–6(a)], whereas in H_2^+ at $R_c=7$ a.u., $8U_p$ electrons are more probable than $10U_p$ electrons [Figs. 1(b) 3(b), and 5(b)], whereas the inverse occurs in Fig. 4(b) for H_2^+ and Fig. 8(a) for H_3^{2+}. However, we note that in all cases the effect of moving nuclei due to Coulomb explosion results in fine structure of each ATI peak with equalization of the intensities of these ATI peaks in the energy region $E\geqslant2U_p$.

It is to be expected that ionizing electrons that leave the molecule at the critical internuclear distance R_c at which CREI occurs will find the molecular ion core at larger internuclear distance $R>R_c$ since the H_2^+ or H_3^{2+} will be undergoing Coulomb explosion, (CE), which can be used as we have shown for dynamic imaging of the nuclear wave functions [16,17]. The time evolution of CE molecular fragments can be modeled using classical mechanics. Assuming that at R_c, ions of charge $+Q$ have zero velocity and initial potential energy $E=Q^2/R_c$, we can calculate the time t to reach distance R by integrating the classical equation of motion $\mu d^2R/dt^2=-Q^2/R^2$, where μ is the molecular reduced mass. We thus obtain [28]

$$t=\left(\frac{\mu}{2}\right)^{1/2}\int_{R_c}^{R}(E-Q^2/R)^{-1/2}dR, \tag{18}$$

$$=\left(\frac{\mu}{2}\right)^{1/2}R_c^{3/2}[x/(x^2-1)-0.5\ln\{(x+1)/(x-1)\}]/Q, \tag{19}$$

where $x=[R/(R-R_c)]^{1/2}$. The first return time is given by the relation $\omega t=1.3\pi$ at initial phase $\phi=0.1\pi$ [14,33], which corresponds to 0.65 cycle of the laser pulse. Thus at $\lambda=1064$ nm, this corresponds to $t=2.31$ fs$=95$ a.u. (1 a.u.$=24.2\times10^{-18}$ s), whereas at 800 nm, $t=1.8$ fs $=74$ a.u. Therefore, recollision and CE occur on near-femtosecond time scale. Inserting $R_c=7$ a.u. at 1064 nm and $R_c=8$ a.u. at 800 nm, we obtain for H_2^+ $(Q=1)$ from Eq. (19) the final distance reached by the Coulomb exploding protons ($R\simeq11$ a.u.) in both cases. This means that the CE displacement is 3 a.u.$\leqslant\Delta R\leqslant4$ a.u. for the protons upon the first recollision of the ionized electron. Since the total phase of the field is $\omega t+\phi=1.4\pi$, where $E(t)=E_0\cos(\omega t+\phi)$, then recollision occurs near zero-field amplitude as indicated above. We conclude therefore that since ionization and therefore CE occurs mainly at R_c, then the above simple calculation shows that recollision diffraction should occur at $R\simeq11$ a.u. for both 1064-nm and 800-nm laser pulses. Using the recollision electron wavelength λ_r at energy πU_p (Tables I and II) gives the ratio $R/\lambda_r\simeq2.75$, 3.2, 3.9, 2.1, 2.9, 4.1 a.u., thus implying near maximum transmission of the recolliding electron through the CE protons. This conclusion correlates well with the observation that the $10U_p$ ATI peak intensities remain strong in the presence of the moving nuclei. However, there is little sensitivity to the intensities, i.e., no marked signature of the wavelength interference effects. This is related, we believe, to the fact that the kinetic energy of the recolliding electron E is much greater than the molecular potential V_0 in Eqs. (16) and (17).

Finally, we comment on the fine structure of the ATI peaks that are accentuated by the moving nuclei, Figs. 1(c)–6(c) and 7(b)–9(b). These structures occur both in the H_2^+ spectra where the initial states are bound vibrational states and in the H_3^{2+} spectra where the initial nuclear state was taken to be a Gaussian wave packet for symmetric dissociation on a repulsive potential. In view of the difference of initial nuclear states for H_2^+ (bound) and H_3^{2+} (dissociative), and yet similarities in the moving nuclei ATI spectra, we conclude that the fine structure is due to electronic resonances in the ATI excitations. Perusal of Fig. 10 for H_3^{2+} at $R=8$ a.u. and intensities 1.0×10^{14} W/cm^2 and Fig. 11 at 2.0×10^{14} W/cm^2 at $\lambda=800$ nm, respectively, shows considerable structure of the static nuclei peaks. The structure becomes more resolved with the moving nuclei as the nuclei probe the varying Franck-Condon factors during the pulse.

As discussed above, displacements $\Delta R \simeq 3-4$ a.u. of protons are expected during the first recollision time of the electron, which is ~ 1.8 fs at 800 nm and is independent of intensity. Figures 10(a) and 11(a) show excellent correlation between the static nuclei ATI subpeaks with the corresponding moving nuclei ATI structure illustrated in Figs. 10(b) and 11(b). In general, similar subpeaks or structures survive in the high-energy ATI spectra, i.e., $8U_p$ and $10U_p$ (see Figs. 1–9), confirming that the same resonances participate in the ionization process.

V. CONCLUSIONS

We have presented ATI spectra of the one-electron systems H_2^+ and H_3^{2+} with static and moving nuclei. Comparison with H atom spectra confirms the role of CREI as the main source of the molecular ionization at the critical internuclear distance $R_c \simeq 7$ a.u., due to a consistent shift of maxima-minima of molecular ATI spectra by the Stark-field energy $E_M R_c/2$, where E_M is the maximum field amplitude. This is the result of the excitation of the LUMO around R_c by the laser, resulting in the electron being transferred from the HOMO to the up-field quasistatic well before it ionizes. This has no equivalent in the atomic case. In the molecular case this results in Stark shifts linear with the field E, whereas in the atomic case such Stark shifts are at least quadratic in the field. Furthermore, this Stark energy effect on the spectra is only operative in the parallel molecule-field configuration [15], and as shown in Tables I and II, it can affect the πU_p recollision energy of an electron by about 20%. Comparison of the moving nuclear (non-Born-Oppenheimer) ATI spectra with the static (Born-Oppenheimer) spectra shows them to be quite similar to the latter at the critical distance R_c where CREI occurs. This confirms that enhanced ionization occurs mainly at R_c. The appearance of fine structure in the moving nuclei spectra suggests that the nuclei are sweeping through different resonances as a function of internuclear distance $R \sim R_c$. Recollision diffractive interference effects are negligible due to two factors:

(a) The high energy, πU_p, of the recolliding electrons with respect to the revisited molecular Coulomb potential V_0 according to the simple single well model, Eqs. (17) and (16). Such a single-well model has been treated in a full Floquet analysis [37] and needs to be extended to multiple wells in order to determine appropriate laser-molecule parameters to enhance recollision diffraction; (b) Moving protons readily change position to $\Delta R \sim 3-4$ a.u. in the first electron recollision that occurs during 0.65 cycles of a laser pulse. Such nuclear displacement can, of course, be avoided by examining heavier and strongly bound molecules such as N_2 [38] or using shorter pulses. Another solution to avoid ''dressing'' of the molecular ion core is to adopt a perpendicular excitation scheme first suggested in Ref. [15] and recently implemented for H_2^+ [39]. In the latter, the effect of electron recollision on the molecular (proton) ATD spectra was measured. Perpendicular and parallel coincidence ATI and ATD spectra would be an important complementary experiment in order to confirm electron recollision diffraction in molecules on near-femtosecond time scale and to exploit LIED as a new tool for measuring molecular dynamics on near-femtosecond, and even near-attosecond, time scales.

ACKNOWLEDGMENTS

We thank the NSERC (Natural Sciences and Engineering Research Council of Canada) and the CIPI (Canadian Institute for Photonics Innovations) for financial support of this work. We also acknowledge ''illuminating'' discussions on LIED with P. B. Corkum (Ottawa).

[1] T. Brabec and F. Krausz, Rev. Mod. Phys. **72**, 545 (2000).
[2] M. Gavrila, *Atoms in Intense Laser Fields* (Academic Press, New York, 1992).
[3] A.D. Bandrauk and E. Constant, J. Phys. **1**, 1033 (1991).
[4] C. Wunderlich, E.K. Kobler, H. Figger, and T. Hansch, Phys. Rev. Lett. **78**, 2333 (1997).
[5] A.D. Bandrauk, *Molecules in Laser Fields* (Dekker, New York, 1994), Chap. 1.
[6] S. Chelkowski, T. Zuo, O. Atabek, and A.D. Bandrauk, Phys. Rev. A **52**, 2977 (1995).
[7] S. Chelkowski, C. Foisy, and A.D. Bandrauk, Phys. Rev. A **57**, 1176 (1998); Int. J. Quantum Chem. **65**, 503 (1997).
[8] A.D. Bandrauk, in *The Physics of Electronic and Atomic Collisions*, edited by Yukikazu Itikawa, Kazuhiko Okuno, Hiroshi Janaka, Akira Yagishita, and Michio Matsuzawa, AIP Conf. Proc. 500 (AIP, Melville, NY, 2000), p. 102.
[9] H. Yu and A.D. Bandrauk, Phys. Rev. A **59**, 539 (1999); J. Phys. B **31**, 4243 (1998); A. D. Bandrauk, S. Chelkowski, H. Yu, and E. Constant, Phys. Rev. A **56**, R2537 (1997).
[10] J. Verschuur, L.D. Noordam, and H.B. van Linden van den Heuvell, Phys. Rev. A **40**, 4383 (1989).
[11] A. Zavriyev, P.H. Bucksbaum, H.G. Muller, and D.W. Schumacher, Phys. Rev. A **42**, 5500 (1990).
[12] P. Salieres *et al.*, Science **292**, 902 (2001).
[13] A. Lohr, M. Kleber, R. Kopold, and W. Becker, Phys. Rev. A **55**, R4003 (1997).
[14] P.B. Corkum, Phys. Rev. Lett. **73**, 1994 (1993).
[15] T. Zuo, A.D. Bandrauk, and P.B. Corkum, Chem. Phys. Lett. **259**, 313 (1996).
[16] A.D. Bandrauk and S. Chelkowski, Phys. Rev. Lett. **87**, 273004 (2001); Chem. Phys. Lett. **336**, 518 (2001).
[17] S. Chelkowski and A.D. Bandrauk, Phys. Rev. A **65**, 023403 (2002).
[18] C.A. Coulson, Trans. Faraday Soc. **33**, 1470 (1937).
[19] H.D. Cohen and U. Fano, Phys. Rev. **150**, 30 (1966).
[20] F. Grasbon *et al.*, Phys. Rev. A **63**, 041402 (2001).
[21] P. Dietrich, P.B. Corkum, D.T. Strickland, and M. Lagerge, in *Molecules in Laser Fields*, edited by A.D. Bandrauk (Dekker, New York, 1994), Chap. 4.
[22] J.R. Hiskes, Phys. Rev. **122**, 1207 (1961).
[23] H. Yu, T. Zuo, and A.D. Bandrauk, Phys. Rev. A **54**, 3290

(1996); H. Yu and A.D. Bandrauk, *ibid.* **56**, 685 (1997); H. Yu and A.D. Bandrauk, J. Chem. Phys. **102**, 1257 (1995).
[24] I. Kawata, H. Kono, and A.D. Bandrauk, Phys. Rev. A **64**, 043411 (2001); I. Kawata, H. Kono, Y. Fujimura, and A.D. Bandrauk, *ibid.* **62**, 031401 (2000).
[25] A.D. Bandrauk and H. Shen, J. Chem. Phys. **99**, 1185 (1993); J. Phys. A **27**, 7147 (1994).
[26] F.H.M. Faisal, *Theory of Multiphoton Processes* (Plenum Press, New York, 1987).
[27] A.D. Bandrauk and H.Z. Lu, THEOCHEM **547**, 97 (2001); J. Chem. Phys. **115**, 1670 (2001).
[28] S. Chelkowski and A.D. Bandrauk, J. Phys. B **28**, L723 (1995).
[29] T. Zuo, S. Chelkowski, and A.D. Bandrauk, Phys. Rev. A **49**, 3943 (1994); T. Zuo and A.D. Bandrauk, *ibid.* **52**, R2511 (1995).
[30] T. Seideman, M. Ivanov, and P.B. Corkum, Phys. Rev. Lett. **75**, 2819 (1995).
[31] M.J. Dewitt, E. Wells, and R.R. Jones, Phys. Rev. Lett. **343**, 345 (2001).
[32] A. Becker, S.L. Chin, and A.D. Bandrauk, Chem. Phys. Lett. **343**, 345 (2001).
[33] K.J. LaGattuta and J.S. Cohen, J. Phys. B **31**, 5281 (1998).
[34] I. Kawata, H. Kono, and Y. Fujimura, Chem. Phys. Lett. **289**, 546 (1998).
[35] H.Z. Lu and A.D. Bandrauk, Phys. Rev. A **62**, 053406 (2000).
[36] T. Taylor, *Mechanics: Classical and Quantum* (Plenum Press, New York, 1976), p. 198.
[37] W.S. Truscott, Phys. Rev. Lett. **70**, 1900 (1993).
[38] A.D. Bandrauk, D.G. Musaev, and K. Morokuma, Phys. Rev. A **59**, 4309 (1999).
[39] H. Niikura *et al.*, Nature (London) **417**, 917 (2002).